

A Systems Model of Vesicle Trafficking in Arabidopsis Pollen Tubes^{[W][OA]}

Naohiro Kato*, Hongyu He, and Alexander P. Steger

Department of Biological Sciences (N.K., A.P.S.) and Department of Mathematics (H.H.), Louisiana State University, Baton Rouge, Louisiana 70803

A systems model that describes vesicle trafficking during pollen tube growth in Arabidopsis (*Arabidopsis thaliana*) was constructed. The model is composed of ordinary differential equations that connect the molecular functions of genes expressed in pollen. The current model requires soluble N-ethylmaleimide-sensitive fusion protein attachment protein receptors (SNAREs) and small GTPases, Arf or Rab, to reasonably predict tube growth as a function of time. Tube growth depends on vesicle trafficking that transports phospholipid and pectin to the tube tip. The vesicle trafficking genes identified by analyzing publicly available transcriptome data comprised 328 genes. Fourteen of them are up-regulated by the gibberellin signaling pathway during pollen development, which includes the SNARE genes *SYP124* and *SYP125* and the Rab GTPase gene *RABA4D*. The model results adequately fit the pollen tube growth of both previously reported wild-type and *raba4d* knockout lines. Furthermore, the difference of pollen tube growth in *syp124/syp125* single and double mutations was quantitatively predicted based on the model analysis. In general, a systems model approach to vesicle trafficking arguably demonstrated the importance of the functional connections in pollen tube growth and can help guide future research directions.

During pollination, when the pollen-stigma interaction is compatible, pollen cells grow a long tube to deliver sperm to the ovule. This polarized growth largely depends on vesicle trafficking that regulates the flow of macromolecules, such as phospholipids and polysaccharides, to the tip of the pollen tube. Studies investigating vesicle trafficking in pollen tubes of tobacco (*Nicotiana tabacum*) and lily (*Lilium longiflorum*) revealed the importance of spatial and temporal changes (Moscatelli et al., 2007; Bove et al., 2008; Zonia and Munnik, 2008) as well as the cytoskeletal and calcium regulations (Cai and Cresti, 2009) of vesicles during the period of polarized growth.

On the other hand, transcriptome analysis revealed genes expressed in Arabidopsis (*Arabidopsis thaliana*) pollen. Four independent studies reported that pollen of Arabidopsis express approximately 30% of genes encoded in the genome (Honys and Twell, 2004; Pina et al., 2005; Borges et al., 2008; Wang et al., 2008). Gene ontology analysis of these transcriptome data demonstrated that the expressed genes in pollen are enriched with vesicle trafficking machinery (Pina et al., 2005). In addition to these studies, transcriptome studies addressing hormone signaling pathways in pollen de-

velopment and pollen tube growth have been conducted in Arabidopsis and rice (*Oryza sativa*; Achard et al., 2004; Cheng et al., 2004; Kaneko et al., 2004; Tsuji et al., 2006; Allen et al., 2007). GA regulates cell growth and development in plants (Silverstone et al., 1997). Several independent studies showed that loss-of-function mutations in the GA signaling pathway impaired pollen development and tube growth in both Arabidopsis and rice. For instance, *ga1-3*, a GA-deficient Arabidopsis mutant, exhibits a defect in pollen maturation and also shows retarded vegetative growth (Silverstone et al., 1997). In addition, genetic analyses of the GA signaling pathway, namely DELLA (a negative regulator of GA signaling) and GAMYB (a positive regulator of GA signaling) knockouts (Achard et al., 2004; Cheng et al., 2004), and ectopic expression of microRNA (*35S:miR159a* suppresses the expression of GAMYB in pollen; Achard et al., 2004; Allen et al., 2007) demonstrated that loss-of-function mutations in the GA signaling pathway impaired pollen development and pollen tube growth in Arabidopsis. Similarly, genetic analyses of the GA signaling pathway in rice, namely the GAMYB loss-of-function mutation (*gamyb*; Kaneko et al., 2004) and miR159 ectopic expression (*POsACT1:miR159*; Tsuji et al., 2006), showed that the GA signaling pathway regulates rice pollen development as well. Furthermore, analysis of the KAO missense mutation, one of the GA synthesis proteins, has demonstrated defective pollen tube growth in rice (Chhun et al., 2007). These studies suggest that the GA signaling pathway may regulate pollen tube growth in both Arabidopsis and rice.

Pollen cells are enclosed by a phospholipid bilayer (plasma membrane) and a cell wall (polysaccha-

* Corresponding author; e-mail kato@lsu.edu.

The author responsible for distribution of materials integral to the findings presented in this article in accordance with the policy described in the Instructions for Authors (www.plantphysiol.org) is: Naohiro Kato (kato@lsu.edu).

^[W] The online version of this article contains Web-only data.

^[OA] Open Access articles can be viewed online without a subscription.

www.plantphysiol.org/cgi/doi/10.1104/pp.109.148700

rides). The cells also have the endomembrane system, including organelles such as the endoplasmic reticulum (ER), Golgi apparatus, endosome, and vacuole, which are also enclosed by a phospholipid bilayer. During pollen tube growth, several molecules required for pollen tube growth, such as proteins, phospholipids, and polysaccharides, are produced, stored, or transported in these organelles. At the tube tip, phospholipids are incorporated into the plasma membrane while polysaccharides such as pectin are incorporated into the cell wall (Samaj et al., 2006; Lee and Yang, 2008). In order to transport these molecules (cargos) among the organelles and to the tube tip (compartments hereafter), vesicles bud from a compartment membrane and traffic in the cytosol. When a vesicle arrives at its destination, the vesicle membrane fuses to the destination membrane and releases its cargo into or onto the compartment membrane.

Studies on vesicle trafficking in yeast and animals have demonstrated that the minimum requirement for protein budding and vesicle fusion is small GTPases, namely Arf or Rab, and soluble *N*-ethylmaleimide-sensitive fusion protein attachment protein receptors (SNAREs; Seabra and Wasmeier, 2004; Behnia and Munro, 2005; Hofmann et al., 2006; Cai et al., 2007; Markgraf et al., 2007). During vesicle budding, a small GTPase located on a compartment membrane recruits machinery proteins, such as coat proteins, from the cytosol. These machinery proteins generate vesicles from the compartment membrane. At the same time, the small GTPase initiates the recruitment of vesicle (v)-SNAREs localized in the compartment membrane and cargos into the vesicle through a cascade of protein interactions. While a vesicle travels within the cytosol, a small GTPase on the vesicle membrane may be converted to the other small GTPase that defines the vesicle destination through a series of protein interactions (Grosshans et al., 2006). Meantime, v-SNARE and the cargo remain in the vesicle. When the vesicle reaches its destination, v-SNAREs interact with target (t)-SNAREs in the compartment membrane (Sorensen et al., 2006). This interaction facilitates vesicle fusion using energy generated between v-SNAREs and t-SNAREs (Stein et al., 2009). To date, more than 15 different gene families whose products are part of a complex machinery of vesicle trafficking have been identified (Schmid and McMahon, 2007). Although not included in the vesicle trafficking family in the strict sense, cytoskeletal proteins such as actins, myosins, microtubules and dyneins are also known to play an important role in vesicle transportation within the cytosol in yeast and animals (Ridley, 2006). Because plant genomes encode homologs of all of these genes, it has been suggested that the basic mechanism of vesicle trafficking in plants is similar to that of yeast and animals (Sanderfoot and Raikhel, 2003; Samaj et al., 2005; Lam et al., 2007; Paul and Frigerio, 2007; Otegui and Spitzer, 2008; Robinson et al., 2008; Rojo and Denecke, 2008).

Direct evidence that shows the importance of vesicle trafficking machinery in pollen tube growth has been mainly reported using gene knockout in *Arabidopsis*, where pollen tube growth is impaired either *in vitro* or *in vivo*. These include knockouts of small GTPase (Szumlanski and Nielsen, 2009), phosphatidylinositol (PI) kinase (Ischebeck et al., 2008; Lee et al., 2008; Sousa et al., 2008), vesicle tethering factor (Cole et al., 2005), vacuolar membrane protein (Fujiki et al., 2007), and vesicle coat protein (Van Damme et al., 2006). However, the fundamental question of how these gene products lead to pollen tube growth remains unanswered.

Systems biology views a biological process as a complex system rather than trying to reduce or simplify the process into discrete elements (Kitano, 2002). A central goal of systems biology is to construct a mathematical model that predicts the outcome of a biological process of interest. Because genes expressed in *Arabidopsis* pollen tubes have been identified and the system outcome (tube growth) can be quantitatively measured (both *in vitro* and *in vivo*) as a function of time, this process represents an ideal arena in which to take full advantage of a systems biology approach and the rich genetic materials to answer fundamental questions. Here, we present such a mathematical model that connects the molecular functions of genes expressed in *Arabidopsis* pollen tubes.

RESULTS AND DISCUSSION

Transcriptome Analysis Elucidates Genes Encoding the Machinery of Vesicle Trafficking in *Arabidopsis* Pollen

To construct a mathematical model that is capable of being evaluated genetically, we sought to define genes of the vesicle trafficking machinery in *Arabidopsis* pollen tubes. In *Arabidopsis*, four independent studies on transcriptional profiling of pollen using the same microarray format (Affymetrix *Arabidopsis* ATH1 Genome Arrays) have been reported (Honys and Twell, 2004; Pina et al., 2005; Borges et al., 2008; Wang et al., 2008). The array contained a 22,591-probe set, which represented approximately 75% of the annotated genes in the *Arabidopsis* genome (Wang et al., 2008). All studies came to a similar conclusion that approximately 30% of the genes probed on the array (about 6,500 genes) were expressed in mature pollen or pollen tubes.

Among these transcriptome data, we used the data published by Pina et al. (2005), Honys and Twell (2004), and Borges et al. (2008), in which transcriptions in mature pollen are compared with those in other cell types such as leaf and root. First, we listed 18 *Arabidopsis* gene families whose orthologs in yeast and animals are known to compose the vesicle trafficking machinery. These include small GTPase (Vernoud et al., 2003), GAP (GTPase-activating protein; Vernoud et al., 2003), GDI (guanine nucleotide dissociation

inhibitor; Vernoud et al., 2003), GEF (guanine nucleotide exchange factor; Vernoud et al., 2003; Anders and Jurgens, 2008), clathrin (Sanderfoot and Raikhel, 2003), adaptins (Sanderfoot and Raikhel, 2003), COP (Sanderfoot and Raikhel, 2003; Paul and Frigerio, 2007), retromer (Sanderfoot and Raikhel, 2003; Paul and Frigerio, 2007), ENTH (epsin N-terminal homology; Paul and Frigerio, 2007), exocyst (Elias et al., 2003), SNARE (Sanderfoot and Raikhel, 2003; Yoshizawa et al., 2006), and PI metabolic pathway enzymes (Lin et al., 2004). These have a total of 360 gene members (Table I; Supplemental Table S1). Within these 360 gene members, we found that 328 genes are expressed at statistically high levels (detection call in the Affymetrix analysis is present) in pollen, sperm, seedling, silique, cotyledon, leaf, petiole, stem, root, or root hair zone (Supplemental Table S1). We then categorized these genes into four groups: (1) “present” in pollen; (2) “enriched” (expression in pollen is at least 1.2-fold higher than that in the other tissues); (3) “selectively expressed” (detection call is present in pollen but absent in the other tissues); and (4) “absent” (detection call is absent in pollen but present at least in one of the other tissues).

This categorization revealed that 49% (161 of 328) of the genes are present and 51% (167 of 328) of the genes are absent in pollen (Fig. 1). Of these present genes in pollen, 13% (42 of 328) are enriched or selectively expressed in pollen (Fig. 1). This suggests that a unique set of genes, which are not expressed or are

expressed at very low levels in other tissues, is involved in vesicle trafficking of Arabidopsis pollen tube growth.

Gene Expression of Selected Small GTPases and SNAREs Is Controlled by the GA Signaling Pathway in Pollen

Next, we sought to identify mutant Arabidopsis lines in which the vesicle trafficking genes expressed in pollen are down-regulated, so that we might be able to find an upstream gene(s) that regulates the expression of vesicle trafficking genes in pollen. To identify mutant lines, we used the 161 vesicle trafficking genes expressed in pollen (Fig. 1; Supplemental Table S1) as queries in analysis by Genevestigator (Hruz et al., 2008). This analysis revealed two related mutant lines in which the same cluster of vesicle trafficking genes is clearly down-regulated (less than 0.5-fold) in flower tissues (including pollen) compared with the wild type (Table II). The two related mutant lines identified are *gal1-3* and *35S:miR159a*. We also found that the genes in the cluster were down-regulated in a *penta* mutant (Cao et al., 2006), in which *gal1-3* and the members of the DELLA gene family are knocked out (Table II). The number of genes in the cluster is 14 (Fig. 1; Table II). Of these, 10 genes belong to the Rab GTPase gene family (and Rab GDI and Arf GAP) or SNARE gene family (Table II). Three genes belong to the exocyst family, and one gene belongs to the PI

Table I. Gene families of vesicle trafficking machinery

Gene families that are known to compose the vesicle trafficking machinery in yeast and animals are listed. The family members in Arabidopsis were identified by different research groups (indicated in the “Reference” column). The numbers of each family member are listed in the “Members” column. The numbers of the members whose expression is enriched (expressed at least 1.2-fold higher than other tissues) or selective (Affymetrix detection call is present only in pollen) are listed in the “Pollen Enriched or Selective” column. The analysis was based on the data of Honys and Twell (2004), Pina et al. (2005), and Borges et al. (2008). The numbers of members whose expression is down-regulated (less than 0.5-fold) in flower tissues (including pollen) of both *gal1-3* (Cao et al., 2006) and *35S:mir159a* (Schwab et al., 2005) mutants are listed in the “GA Down” column. The down-regulated genes were identified by Genevestigator V3 (Hruz et al., 2008) with its default setting.

| Kato Identifier | Family | Reference | Members | Pollen Enriched or Selective | GA Down |
|-----------------|------------------|--|---------|------------------------------|---------|
| 1 | Rab GTPase | Vernoud et al. (2003) | 57 | 8 | 4 |
| 2 | Arf GTPase | Vernoud et al. (2003) | 21 | 1 | 0 |
| 3 | Arf GAP | Vernoud et al. (2003) | 15 | 4 | 1 |
| 4 | Rab GDI | Vernoud et al. (2003) | 4 | 1 | 1 |
| 5 | Rab GEF | Vernoud et al. (2003) | 2 | 0 | 0 |
| 6 | Rab GAP | Vernoud et al. (2003) | 20 | 1 | 0 |
| 7 | Arf GEF | Anders and Jurgens (2008) | 8 | 1 | 0 |
| 8 | Clathrin | Sanderfoot and Raikhel (2003) | 4 | 0 | 0 |
| 9 | Adaptins | Boehm and Bonifacino (2001) | 20 | 0 | 0 |
| 10 | COPII coat | Sanderfoot and Raikhel (2003) and Paul and Frigerio (2007) | 13 | 0 | 0 |
| 11 | COPI compartment | Sanderfoot and Raikhel (2003) and Paul and Frigerio (2007) | 14 | 0 | 0 |
| 12 | Retromer | Sanderfoot and Raikhel (2003) and Paul and Frigerio (2007) | 9 | 0 | 0 |
| 13 | ENTH | Paul and Frigerio (2007) | 3 | 1 | 0 |
| 14 | Exocyst | Elias et al. (2003) | 30 | 3 | 3 |
| 15 | ROP GTPase | Vernoud et al. (2003) | 11 | 3 | 0 |
| 16 | RAN GTPase | Vernoud et al. (2003) | 4 | 0 | 0 |
| 17 | PI enzymes | Lin et al. (2004) | 61 | 9 | 1 |
| 18 | SNARE | Sanderfoot and Raikhel (2003) and Yoshizawa et al. (2006) | 64 | 10 | 4 |
| Total | 18 | | 360 | 42 | 14 |

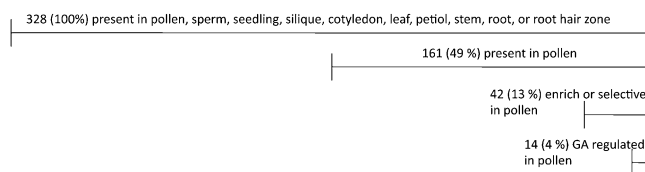


Figure 1. Numbers and percentages of vesicle trafficking genes that are present, enriched, or selectively expressed in Arabidopsis pollen. A total of 328 vesicle trafficking genes that are expressed at statistically high levels (detection call in the Affymetrix analysis is present) in pollen, sperm, seedling, silique, cotyledon, leaf, petiole, stem, root, or root hair zone were analyzed (Honys and Twell, 2004; Pina et al., 2005; Borges et al., 2008). Enriched indicates genes that express in pollen at least 1.2-fold higher than in other tissues (Honys and Twell, 2004; Pina et al., 2005; Borges et al., 2008). Selective indicates genes whose detection call is present in pollen but absent in the other tissues. GA regulated indicates genes whose expression is down-regulated in Arabidopsis mutants of the GA signaling pathway identified by Genevestigator V3 (Hruz et al., 2008). Forty-nine percent of vesicle trafficking genes are present and 51% are absent. Forty-two genes are enriched or selectively expressed in pollen. These data indicate that selected vesicle trafficking genes are used, and 14 of them are up-regulated by the GA signaling pathway, in pollen.

metabolic enzyme family. This suggests that the function of the selected minimum machinery of vesicle trafficking in pollen tube, SNARE and small GTPase, may be controlled by the GA signaling pathway.

Exocyst proteins are a subunit of a tethering complex that functions during vesicle fusion in the plasma membranes of yeast and animals (He and Guo, 2009). In Arabidopsis, a knockout mutant of AtEXP70A1 that is absent in pollen (Supplemental Table S1) shows

defects in the polar growth of root hairs and stigmatic papillae (Synek et al., 2006). Knocking out genes of several other subunits in the tethering complex causes defects in pollen germination and pollen tube growth (Hala et al., 2008). Moreover, in an Arabidopsis knockout mutant of a P-type ATPase cation pump gene that is required for normal pollen development, *male gametogenesis impaired anthers*, expression of the three exocyst genes (AtEXO70H3, AtEXO70C1, and AtEXO70C2) is selectively down-regulated (Jakobsen et al., 2005). These results suggest that exocyst proteins may play an important role in pollen tube growth. Knockout analyses in these genes are required to conclude the finding.

The other gene family identified was the PI metabolic enzyme family, PIP5K10. An Arabidopsis knockout mutant of PIP5K4, which is enriched in pollen (Supplemental Table S1) and mainly localizes in the plasma membrane of a pollen tube tip, impairs pollen tube growth (Sousa et al., 2008). Hence, it is reasonable to assume that expression of an enzyme in the same metabolic pathway controls pollen tube growth. Again, knockout analysis in this gene is required to conclude the finding.

We also analyzed changes of the expression levels in these 14 genes during pollen tube growth based on the data published by Wang et al. (2008). We found that the expression levels of these 14 genes are little changed during pollen tube growth (Wang et al., 2008), suggesting that the vesicle trafficking may be established rapidly before or during pollen germination. Furthermore, we found that 10 of the 14 genes, which are all enriched and selectively expressed in pollen in the data of Pina et al. (2005), are up-regulated

Table II. Vesicle trafficking genes that are down-regulated in Arabidopsis mutants

Genes enriched or selectively expressed in pollen and down-regulated in flower tissues (including pollen) of both *ga1-3* and *35S:miR159a* mutants are listed. "Pollen Selective" and "Pollen Enriched" data are from Pina et al. (2005). "Changed in Growth" indicates that gene expression is down- or up-regulated (at least 1.6-fold difference) during tube growth; data are from Wang et al. (2008). "Penta/Wild Type" shows a relative gene expression level in flower tissues (including pollen) of a *penta* mutant over wild-type Arabidopsis. The *penta* mutant carries five mutations in which *ga1-3* and the members of the DELLA gene family are knocked out (Cao et al., 2006). "HSP90RNAi-A3/Wild Type" shows a relative gene expression level in flower tissues (including pollen) of a *hsp90* knockdown line over wild-type Arabidopsis (Sangster et al., 2007). The data of "Penta/Wild Type" and "HSP90RNAi-A3/Wild Type" are from Genevestigator V3 (Hruz et al., 2008). "Reported" indicates that defective pollen tube growth in a knockout line was reported previously (Boavida et al., 2009; Szumlanski and Nielsen, 2009).

| Kato Identifier | Family | Annotation | Arabidopsis Genome Initiative No. | Pollen Selective | Pollen Enriched | Changed in Growth | Penta/Wild Type | HSP90RNAi-A3/Wild Type | Reported |
|-----------------|------------|------------|-----------------------------------|------------------|-----------------|-------------------|-----------------|------------------------|----------|
| 1 | Rab GTPase | AtRABA1i | AT1G28550 | Yes | Yes | No | 0.43 | 5.98 | No |
| 1 | | AtRABA4d | AT3G12160 | Yes | Yes | No | 0.15 | 3.86 | Yes |
| 1 | | AtRABH1d | AT2G22290 | Yes | Yes | No | 0.64 | 3.73 | No |
| 1 | | AtRABH1e | AT5G10260 | No | Yes | No | 0.71 | 0.74 | No |
| 3 | Aft GAP | AtAGD10 | AT2G35210 | No | Yes | No | 0.53 | 8.36 | Yes |
| 4 | Rab GDI | AtRabGDI3 | AT5G09550 | No | Yes | No | 0.55 | 0.48 | No |
| 14 | Exocyst | AtEXO70H3 | AT3G09530 | Yes | Yes | No | 0.39 | 10.55 | No |
| 14 | | AtEXO70C1 | AT5G13150 | Yes | Yes | No | 0.47 | 3.52 | No |
| 14 | | AtEXO70C2 | AT5G13990 | Yes | Yes | No | 0.61 | 11.73 | No |
| 17 | PI enzymes | PIP5K10 | AT1G01460 | Yes | Yes | No | 0.41 | 2.76 | No |
| 18 | SNARE | SYP125 | AT1G11250 | Yes | Yes | No | 0.54 | 1.6 | No |
| 18 | | AtSNAP30 | AT1G13890 | Yes | Yes | No | 0.36 | 2.05 | No |
| 18 | | SYP131 | AT3G03800 | Yes | Yes | No | 0.59 | 9.29 | No |
| 18 | | SYP72 | AT3G45280 | Yes | Yes | No | 0.41 | 2.57 | No |

in seedlings of the HSP90RNAi-A3 line (Table II; Sangster et al., 2007). In animals, HSP90 is known to regulate Rab GTPase recycling in vesicle trafficking (Chen and Balch, 2006). Although the exact reason for up-regulation of these genes in seedlings is not yet clear, we speculate that when the HSP90 protein is expressed at a certain low level in seedlings, a positive feedback to the gene expression may occur to maintain normal vesicle trafficking.

Among these 14 genes, AtRABA4d and AtAGD10 (Table II) knockout mutations already have been shown to impair pollen tube growth (Boavida et al., 2009; Szumlanski and Nielsen, 2009). Hence, we believe that this transcriptome analysis elucidated key vesicle trafficking genes that regulate pollen tube growth, even if not all vesicle trafficking genes were identified. This analysis also suggests that the network of molecules that regulates vesicle trafficking through the GA signaling pathway may be decoded by expanding the search to other gene families such as cytoskeletons, calcium channel proteins, and the GA signaling pathway in the future.

A Mathematical Model of Vesicle Trafficking in Pollen Tubes

To study the function of vesicle trafficking machinery at a systems level, we constructed a mathematical model that connects the functions of molecules expressed in pollen tubes, which includes gene products elucidated by the transcriptome analysis, using a set of ordinary differential equations (for details, see "Materials and Methods" and Supplemental Proof S1). Heinrich and Rapoport (2005) originally constructed a model to describe vesicle trafficking between the ER and Golgi apparatus. The model was used to computationally explain what kind of initial conditions satisfy equilibrium (generation of nonidentical compartments: the ER and Golgi apparatus) with limited molecular machinery (SNAREs and coat proteins). We adapted this model to describe vesicle trafficking among the Golgi apparatus, pollen tube tip, and recycling endosome (Samaj et al., 2006; Fig. 2). Because of the geometry of the vesicles and pollen tube, the number of vesicles required to elongate the plasma membrane and construct the cell wall is

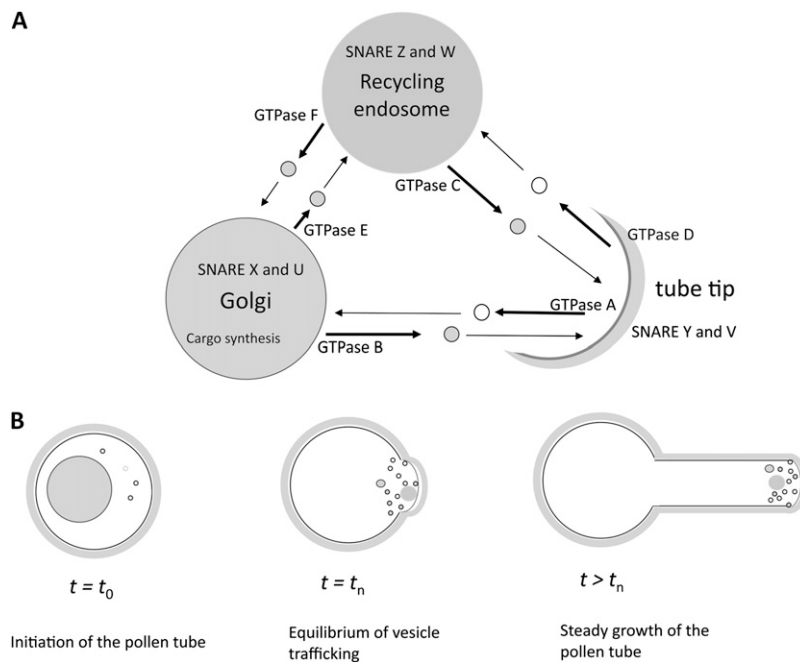


Figure 2. Schematic drawing of a mathematic model of vesicle trafficking in a pollen tube. A, Three-compartment model. We assume that the Golgi apparatus, tube tip, and recycling endosome (large circles and a semicircle) are major compartments that are involved in the transportation of newly synthesized cargos, pectin, and cargo phospholipids (gray) for pollen tube growth. Pectin and cargo phospholipids are de novo synthesized in the Golgi apparatus before tube elongation. These cargos are transported to the tube tip via vesicle (small circles) trafficking established in the pollen. At the tube tip, pectin and cargo phospholipids are incorporated into the plasma membrane and cell wall so that the tube elongates. The majority of SNARE X and U, Y and V, and Z and W localize in the Golgi apparatus, tube tip, and recycling endosome, respectively, when the vesicle trafficking is at equilibrium. GTPase A, B, C, D, E, and F initiate specific vesicle trafficking pathways, as indicated by thick arrows. The cargos are not transported from the tube tip. B, Changes of compartments and cargo transport as a function of time. A pollen tube tip is initiated at time point t_0 . At this point, the vast majority of SNAREs and cargos are in the Golgi apparatus. Vesicle trafficking reaches equilibrium at time point t_n . After this point, the total surface area of the three compartments and numbers of vesicles are not changed. Pectin and cargo phospholipids are transferred by vesicle trafficking even after this time point. For a detailed explanation of this model, see "Materials and Methods" and Supplemental Figures S1 and S2.

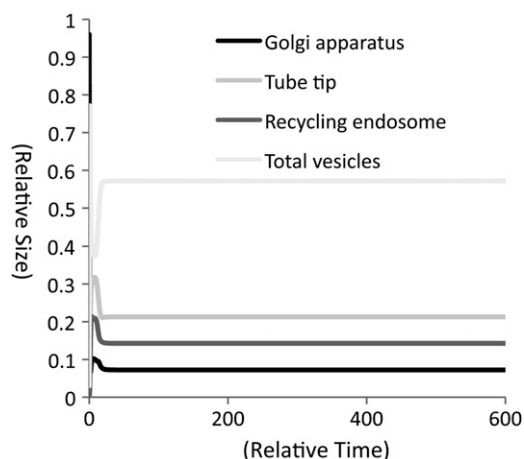


Figure 3. Computational results of changes in areas of the Golgi apparatus, tube tip, recycling endosome, and vesicles as a function of time. The total surface area of the three compartments and vesicles is always 1. The results indicate that the vesicle trafficking reaches equilibrium at t_{25} when it is computed with 0.2 resolution. The results also indicate that the total area of vesicles in a pollen tube is larger than the compartments when the vesicle trafficking is at equilibrium.

thought to be different (Derksen et al., 1995; Bove et al., 2008). In this mathematical model, vesicles are considered as transporters that carry two cargos: (1) phospholipids to expand the plasma membrane, and (2) pectin to construct the cell wall (Supplemental Fig. S1). When a vesicle fuses at the tube tip (exocytosis), phospholipids and pectin are thought to be integrated into the side of the tube where elongation occurs (Supplemental Fig. S2). In biological samples, phospholipids are also used for the vesicle trafficking system (Carr and Novick, 2000). In the model, phospholipids that are used for tube elongation (designated cargo phospholipids) and for the vesicle trafficking system are distinguished (Supplemental Fig. S1). Therefore, the number of vesicles required

to expand the plasma membrane and construct the cell wall is equal but the number of cargo phospholipids and pectins that each vesicle carries is different (Supplemental Fig. S3, A and B). Furthermore, frequencies of exocytosis and endocytosis at the tube tip simply rely on the interaction between cognate v-SNAREs and t-SNAREs and the activities of small GTPase (Arf or Rab GTPase), similar to vesicle budding and fusion at the ER and Golgi apparatus (Supplemental Fig. S3C).

Previously, Heinrich and Rapoport (2005) quantified the parameter values that mathematically satisfied the conditions to maintain nonidentical compartments. Hence, we applied these parameter values in our model (for details, see “Materials and Methods”).

Equilibrium Status of Vesicle Trafficking in a Computed Pollen Tube

First, we mathematically proved that these three compartments (the Golgi apparatus, tube tip, and recycling endosome) can reach equilibrium (generation of nonidentical compartments) with the parameter values we used (Supplemental Proof S1). We subsequently applied the equations to the XPPAUT (for X-Windows Phase Plane plus Auto) program that solves differential equations based on our assumptions regarding pollen tube growth (Supplemental Program S1). The model was run for 600 time steps ($t_0 \leq t \leq t_{600}$) with a resolution of 0.2. The total relative area of compartments and vesicles is always 1 in the model (Supplemental Proof S1; Supplemental Program S1). The computational results indicated that vesicle trafficking reaches equilibrium at t_{25} . At the equilibrium, the relative area of the Golgi apparatus, in which the vast majority of membranes and SNAREs of the vesicle trafficking system are accumulated at t_0 , is reduced from 0.96 (t_0) to 0.07 (t_{25}). At the same time, relative areas of the tube tip and recycling endosome increase from 0.005 (t_0) to 0.21 (t_{25}) and 0.14 (t_{25}),

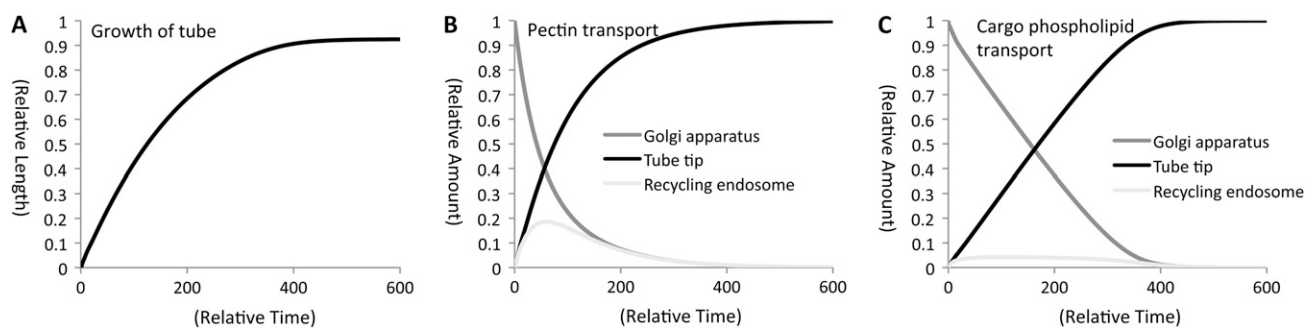


Figure 4. Computational results of changes in pollen tube length and amounts of pectin or cargo phospholipids as a function of time. A, Changes of pollen tube length. The maximum relative length of a pollen tube is 1. B, Changes of pectin amount in the Golgi apparatus, tube tip, and recycling endosome. A total relative amount of pectin is always 1. C, Changes of phospholipid amount in the Golgi apparatus, tube tip, and recycling endosome. The total relative amount of pectin is always 1. The results indicate that a pollen tube grows logarithmically due to logarithmic transport of pectin and nearly linear transport of cargo phospholipids to the tube tip.

Table III. Biological data adapted for computational estimates and predictions

*, Data are from Ketelaar et al. (2008). **, Data are from Boavida and McCormick (2007).

| Vesicle Surface Area* | Tube Diameter* | Maximum Tube Length** | Growing Time** | Tube Tip Surface Area* |
|-----------------------|----------------|-----------------------|----------------|------------------------|
| μm^2 | μm | μm | h | μm^2 |
| 0.10 | 4.53 | 1,000 | 16 | 32.23 |

respectively (Fig. 3). The relative total area of vesicles increases from 0.03 at t_0 to 0.57 at t_{25} (Fig. 3). This indicated that the majority of the surface area required for vesicle trafficking is in vesicles at equilibrium.

Computed Pollen Tube Growth Is Similar to Biological Observations

Next, we computed changes in the length of a pollen tube (Fig. 4A), amounts of pectin (Fig. 4B), and cargo phospholipids (Fig. 4C) in the Golgi apparatus, tube tip, and recycling endosome as a function of time. In the model, the maximum length of the pollen tube and total amount of pectin and cargo phospholipids are all set to 1. The computational growth curve of the pollen tube is logarithmic. The length reaches 0.924 at t_{524} and hardly changes after this time point. This is due to a logarithmic transport of pectin and nearly linear transport of cargo phospholipids at the tube tip. Pectin in the recycling endosome increases until t_{60} (the relative amount is 0.19) and gradually decreases thereafter. Meantime, cargo phospholipids in the recycling endosome rarely increase over time. Logarithmic growth of in vitro-grown pollen was reported previously (Boavida and McCormick, 2007), which supports the results of this model.

To change these relative numbers to absolute numbers, we used previously published data in which areas of vesicles and pollen tubes of Arabidopsis are measured by a transmission electron microscope (Table III; Ketelaar et al., 2008). According to the data, the diameter of a vesicle is $0.182 \mu\text{m}$; hence, the surface area of a vesicle is calculated at $0.10 \mu\text{m}^2$. The average diameter of pollen tubes is $4.53 \mu\text{m}$. We assumed that the shape of the tube tip is a hemisphere with a diameter of $4.53 \mu\text{m}$. Thus, the calculated surface area of the tip tube is $32.23 \mu\text{m}^2$. Based on these measurements, we estimated

that the total membrane area of the vesicle trafficking system among the three compartments is $153.48 \mu\text{m}^2$. At equilibrium, the areas of Golgi apparatus and recycling endosome are 10.74 and $21.49 \mu\text{m}^2$, respectively (Table IV). The surface distributions in the Golgi apparatus and recycling endosome in Arabidopsis pollen have not been obtained. To determine if the model quantitatively predicts these values, an additional series of experiments needs to be conducted. On the other hand, Ketelaar et al. (2008) estimated, based on electron micrographs, that 1,486 vesicles would be present near the tube tip (Table IV). The number of estimated vesicles is 877 at equilibrium. This suggests that the estimated number of the computed vesicles is underestimated. However, this is probably due to the difference in the measurements between the model and the biological sample. The biological sample contains multiple compartments such as the ER and the vacuole (Derksen et al., 2002; Ketelaar et al., 2008) that are not part of the systems model.

We also did comparisons with other previously published biological data in which the lengths of Arabidopsis pollen tubes are measured in vitro as a function of time. The maximum length of in vitro-grown pollen tubes varied from 250 to $1,000 \mu\text{m}$, depending on conditions (Boavida and McCormick, 2007; Ketelaar et al., 2008; Szumlanski and Nielsen, 2009). Given these data, we assumed that the maximum length of pollen is $1,000 \mu\text{m}$ at 16 h when pollen is grown in vitro under optimum conditions (Boavida and McCormick, 2007). Because we computed time from t_0 to t_{600} , we assumed that a single time unit represents 1.6 min in the model. Based on these measurements and assumptions, we estimated that vesicle trafficking in a pollen tube reaches equilibrium within 40 min ($1.6 \text{ min} \times 25$) after the initiation of the pollen tube tip (t_0). We also calculated the growth rate of the pollen tube as it grows from 10 to $100 \mu\text{m}$. The rates were measured in in vitro-grown Arabidopsis pollen (Szumlanski and Nielsen, 2009). We found that the average growth rate of pollen tubes is $3.12 \pm 0.52 \mu\text{m min}^{-1}$ (from 2.8 to $5.9 \mu\text{m min}^{-1}$) in our model (Table IV). Ketelaar et al. (2008) and Szumlanski and Nielsen (2009) report that the growth rate of in vitro-grown Arabidopsis pollen is 4.07 ± 0.36 and $4.5 \pm 1.0 \mu\text{m min}^{-1}$, respectively. These numbers indicate a reasonable agreement between computational estimates and biological observations in pollen tube growth.

Table IV. Data comparisons between biological observations and computational estimates

*, Data are from Ketelaar et al. (2008). **, Data are from Szumlanski and Nielsen (2009). ***, Estimated when the vesicle trafficking is at equilibrium. ****, Estimated when a computed tube length is from 10 to $100 \mu\text{m}$. n/a, Not available.

| Source | Golgi Apparatus | Recycling Endosome | Vesicle Nos. | Tube Growth Rate |
|------------------------|-----------------|--------------------|--------------|------------------------|
| | μm^2 | μm^2 | | $\mu\text{m min}^{-1}$ |
| Biological observation | n/a | n/a | 1,486* | 4.0* or 4.5** |
| Computational estimate | 10.74 | 21.49 | 877*** | 2.8 to 5.9**** |

Computational Results and Observation of *raba4d* Mutant Phenotypes Are Similar

We then tested whether or not our model could correctly estimate vesicle trafficking in mutated pollen. The growth defect of in vitro-grown pollen tubes in the Arabidopsis *raba4d* knockout line was previously reported (Szumlanski and Nielsen, 2009). Because the closest yeast homologs of AtRabA4d, Ypt31/32, are known to initiate vesicle budding from the trans-Golgi network and direct the vesicles to the plasma membrane (Benli et al., 1996; Jedd et al., 1997), we used the *raba4d* knockout data to compare the function of GTPase B, which initiates vesicle transport from the Golgi apparatus to the tube tip in the mathematical model.

Although Arabidopsis expresses three AtRabA4d paralogous genes, AtRabA4a (71% amino acid identity), AtRabA4b (70% amino acid identity), and AtRabA4c (77% amino acid identity), which are most likely functionally redundant to AtRabA4d, our transcriptome analysis revealed that the three paralogous genes are absent in pollen (Supplemental Table S1). Hence, we hypothesized that AtRabA4d (RabA4d hereafter) is the sole source that functions as GTPase B in pollen. Accordingly, we changed the parameter values that represent the function of GTPase B to 0 (Supplemental Program S1) so that the computational results represent the *raba4d* null mutant. The computational results showed that the average growth rate of the pollen tubes is $0.84 \pm 0.34 \mu\text{m min}^{-1}$ when we measured the same time window as in wild-type pollen (Supplemental Program S1). This suggests that the growth rate would be reduced to 26% (0.84 of 3.12) of the wild-type pollen rate (Table V). This number reasonably agrees with the observation of the Arabidopsis *raba4d* knockout line, in which the pollen tube growth rate is reduced to about 18% of that of wild-type pollen (Szumlanski and Nielsen, 2009).

We also estimated that the length of in vitro-grown pollen tubes of wild-type Arabidopsis is $570 \mu\text{m}$, while the length of *raba4d* knockout pollen is $270 \mu\text{m}$ (48% of wild-type Arabidopsis) at the same time point (Fig. 5; Table V). Szumlanski and Nielsen (2009) show that the average length of in vitro-grown pollen tubes of *raba4d* knockout Arabidopsis is about 45% of the wild-type Arabidopsis length after 24 h of incubation when the

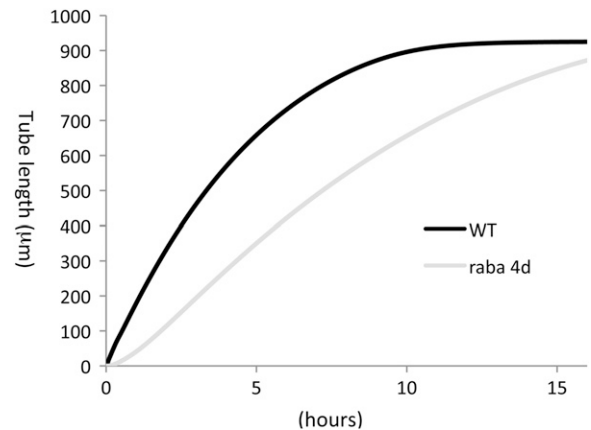


Figure 5. Computational estimations of pollen tube length in wild-type (WT) and *raba4d* knockout Arabidopsis. Changes of pollen tube length in micrometers were estimated as a function of time in hours. The estimations were made by, first, changing computational parameters so that a mathematical function of GTPase B ($w_b = 1$, $1/kxb = 1/kub = 1/kpb = 0.01$, and $1/kyb = 1/kvb = 1/kzb = 1/kwb = 1$) is halted ($w_b = 0$ and $1/kxb = 1/kub = 1/kyb = 1/kvb = 1/kzb = 1/kwb = 1/kpb = 0$) and, second, applying biological data of in vitro-grown wild-type Arabidopsis pollen tubes. The results indicate that when the length of wild-type tubes is $570 \mu\text{m}$, the length of *raba4d* knockout pollen tubes is $270 \mu\text{m}$ (48% of the wild-type value). At 16 h, the length of *raba4d* knockout pollen tubes is 94% of the wild-type pollen.

average length of wild-type Arabidopsis pollen is about $570 \mu\text{m}$. Once again, these numbers indicate that the computational results reasonably agree with observations of the Arabidopsis *raba4d* knockout line. However, the computational results estimated that the length of *raba4d* knockout pollen would be 94% of that of wild-type pollen after 16 h of in vitro culture when the length of wild-type pollen reaches $925 \mu\text{m}$ (Fig. 5). The growth of *raba4d* knockout pollen is indistinguishable from that of wild-type pollen in vivo (Szumlanski and Nielsen, 2009). Therefore, we assume that the length of *raba4d* knockout pollen grown in vitro would not be correctly estimated by our current model. Alternatively, the length of in vitro-grown *raba4d* knockout pollen might become indistinguishable from that of wild-type pollen if pollen is grown under optimum conditions.

Computational Results Predict Localizations of Pectin and SYP125 in *raba4d* Mutant Pollen

We further predicted localizations of SYP125 in the *raba4d* mutant, which have not been investigated in biological samples yet. Our computational results predicted that localizations of SYP125, one of the vesicle machineries regulated by the GA signaling pathway in Arabidopsis pollen (Table II), in the *raba4d* knockout are little different from those in wild-type pollen (Fig. 6A). On the other hand, the amount of pectin transported in the *raba4d* knockout tube tip is reduced to 43% of wild-type pollen (Fig. 6B). This is due to higher recruitment rates of SNAREs to vesicles

Table V. Data comparisons between biological observations and computational estimates in *raba4d* knockout pollen

*, Data are from Szumlanski and Nielsen (2009). **, Estimated in the time window when the length of a computed pollen tube of wild-type Arabidopsis is from 10 to $100 \mu\text{m}$. ***, Estimated when the length of a computed pollen tube of wild-type Arabidopsis is $570 \mu\text{m}$.

| Source | Growth Rate | Tube Length |
|------------------------|-----------------------|-------------|
| | % of wild-type pollen | |
| Biological observation | 18* | 45* |
| Computational estimate | 26** | 48*** |

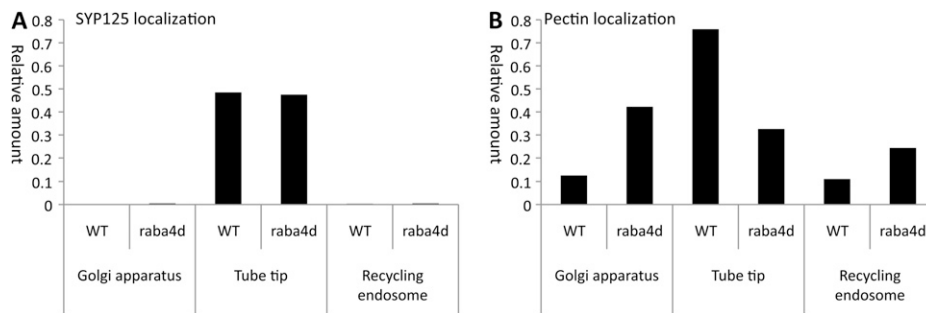


Figure 6. Computational predictions of SYP125 localizations in wild-type (WT) and *raba4d* knockout Arabidopsis. A, Relative amounts of SYP125 that localized in the Golgi apparatus, tube tip, or recycling endosome in a wild-type pollen tube (when the length is 570 μm) or in a *raba4d* knockout pollen tube (when the length is 270 μm). The total relative amount of SYP125 in a pollen is 0.5. B, Relative amounts of pectin that localizes in the Golgi apparatus, tube tip, or recycling endosome in a wild-type pollen tube (when the length is 570 μm) or in a *raba4d* knockout pollen tube (when the length is 270 μm). The total relative amount of pectin in a pollen is 1. The computational results predict that the localization of SYP125 in *raba4d* knockout pollen is almost indistinguishable from that in wild-type pollen, although pectin localization is significantly different.

(i.e. $1/kxe = 1$) than that of pectin (i.e. $1/kpe = 0.01$) in the mathematical model (Supplemental Program S1). In the model, SYP125 is transported into the tube tip soon after the initiation of the tube tip (t_0) through the recycling endosome (Supplemental Fig. S4). Decreased transportation of pectin in the *raba4d* knockout tube tip was already reported (Szumlanski and Nielsen, 2009). It should be possible to test the prediction that the transportation of SYP125 is little different from that of wild-type Arabidopsis by expressing GFP-SYP125 (Enami et al., 2009) in *raba4d* knockout Arabidopsis.

Computational Results Predict a Possible Phenotype of *syp124* and *syp125* Knockout Lines

We also predicted possible phenotypes of *syp125* mutant lines that are not reported yet. We assumed that SYP124 (85% amino acid identity), which is also expressed in pollen, is functionally redundant with SYP125, because these two SNAREs belong to the same Qa subfamily. SYP121 (62% amino acid identity), SYP122 (52% amino acid identity), and SYP123 (63% amino acid identity) also belong to the same Qa subfamily. However, our transcriptome analysis suggested that SYP121, SYP122, and SYP123 are depleted or absent in pollen (Supplemental Table S1). Accordingly, in this prediction, we changed the total amount of SNARE Y from 0.5 to 0.25 or 0 in the model. We assumed that 0.25 represents a *syp125* or *syp124* (single) knockout and 0 represents a *syp124/syp125* (double) knockout mutant. SYP131 (44% amino acid identity), the other Qa subfamily gene, is also highly expressed in mature pollen. However, we did not consider SYP131 as the t-SNARE in the mathematical model, because SYP131 does not show polarized tip localization as SYP124 and SYP125 do (Enami et al., 2009) but rather homogeneous localization in the pollen plasma membrane (Enami et al., 2009). Our current model is limited to only vesicle trafficking to the tube tip, not to the entire plasma membrane.

The results predicted that the length of *syp124* or *syp125* mutant pollen would not be different (99%) from that of wild-type pollen (Fig. 7). However, *syp124/syp125* (double) knockout mutant pollen would be shorter (66% of the wild-type length). This is due to nonlinear algebraic equations in the mathematic model (Supplemental Proof S1). Knockout analyses in these genes are required to test this prediction.

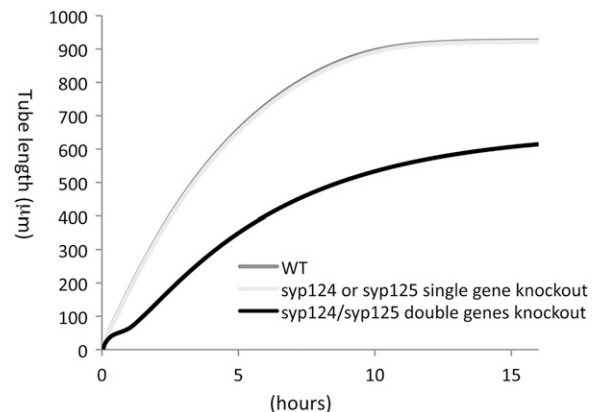


Figure 7. Computational predictions of pollen tube growth in *syp124* and *syp125* knockout Arabidopsis. Changes of pollen tube length in micrometers were predicted as a function of time in hours. The predictions were made by, first, changing computational initial conditions of SNARE Y from $YY1(0) = 0.49$, $YY2(0) = 0.005$, and $YY3(0) = 0.005$ to $YY1(0) = 0.245$, $YY2(0) = 0.0025$, and $YY3(0) = 0.0025$ (representing single gene knockout) or $YY1(0) = 0$, $YY2(0) = 0$, and $YY3(0) = 0$ (representing double gene knockout) and, second, applying biological data of in vitro-grown wild-type (WT) Arabidopsis pollen tubes. The computational results predict that the length of pollen tubes in single gene knockout *syp124* or *syp125* is 99% (922 or 925 μm) of the wild-type pollen when pollen is grown in vitro with the most optimized conditions. On the other hand, the length of pollen tubes in double genes knockout of *syp124* and *syp125* is 66% (614 μm) of the wild-type pollen (925 μm).

REMARKS

We constructed a basic systems model that connects molecular functions of vesicle trafficking genes during pollen tube growth of *Arabidopsis*. We identified 14 genes, 10 of which are small GTPases (and their effectors) or SNAREs, which are up-regulated by the GA signaling pathway during pollen development. The functions of these gene products are used to test or further develop the mathematical model constructed in this study. The computational results of this model, which is limited to connect the functions of small GTPases, SNAREs, and two cargo molecules (pectin and phospholipids), reasonably agree with observations of both wild-type and mutant *Arabidopsis* pollen so far.

We need to test knockout phenotypes of the 14 genes and identify subcellular localizations of their products to clarify the biological functions. The mathematical model reported here does not directly evaluate other vesicle machinery (such as exocyst, PI enzymes, and cytoskeletal proteins), other cargos (such as cellulose synthase), and other compartments (such as the ER, vacuoles, and non-tube-tip plasma membrane) that also should affect pollen tube growth. Moreover, the pollen-stigma interaction and the GA signaling pathway are not incorporated into the model. Therefore, even if our predictions reasonably agree with biological data, this model does not fully represent pollen tube growth or is oversimplified. Lastly, this model does not attempt to actually reflect any biophysical and biomechanical principles of pollen tube growth, such as the mechanics of the cell wall and turgor (Kroeger et al., 2008). While there are limitations to the model, it does connect molecular functions important for pollen tube growth and reasonably predicts the biology of the system. The model can be changed to reflect a variety of complications such as those described above.

MATERIALS AND METHODS

Transcriptome Analyses

Supplemental materials of papers published by Pina et al. (2005), Honys and Twell (2004), and Borges et al. (2008) were used to identify the vesicle trafficking genes that are present in *Arabidopsis thaliana* pollen. Excel files in the supplemental materials were imported to Microsoft Office Access to identify genes in pollen. The vesicle trafficking genes in the list (Supplemental Table S1) were selected based on annotations that were previously published in different papers (Elias et al., 2003; Sanderfoot and Raikhel, 2003; Vernoud et al., 2003; Lin et al., 2004; Yoshizawa et al., 2006; Paul and Frigerio, 2007; Anders and Jurgens, 2008). Genevestigator V3 (Hruz et al., 2008), with its default setting, was used to identify mutants in which a cluster of vesicle trafficking genes are down-regulated. The supplemental material of a paper published by (Wang et al., 2008) was used to analyze changes of expression levels of the selected genes during pollen tube growth.

Mathematical Modeling

The model was constructed based on a model constructed by Heinrich and Rapoport (2005). In our model, we made the following assumptions.

(1) The Golgi apparatus, tube tip, and recycling endosome are defined as compartments 1, 2, and 3, respectively (Fig. 2A).

(2) Vesicle trafficking among these compartments requires v-SNAREs and t-SNAREs for vesicle fusion and small GTPase (Arf or Rab GTPase) for vesicle budding as the minimum machinery (Fig. 2A).

(3) SNARE X and Y, U and V, and Z and W are native to compartments 1, 2, and 3, respectively. t- and v-SNAREs are not distinguishable (i.e. SNARE X and U can be v- or t-SNARE), but their interactions are limited within a pair for their native compartment (i.e. SNARE X interacts with U but not Y, V, Z, and W; Fig. 2A). The total amount of SNARE X, U, Y, V, Z, and W in the cell is 0.5, respectively.

(4) Small GTPase B and E, A and D, and C and F initiate vesicle budding from compartments 1, 2, and 3, respectively (Fig. 2A). These small GTPases also direct the vesicles to a specific compartment via a protein interaction cascade (i.e. GTPase B initiates vesicle budding specifically from compartment 1 and directs the vesicles specifically to compartment 2).

(5) Budding rates are defined by the compartment area and the activity of a specific small GTPase. A direct pathway from the plasma membrane to the Golgi apparatus has not been confirmed in biological samples, although it may exist. Hence, the budding rate of vesicles that transfer from the tube tip to the Golgi apparatus is extremely low. Therefore, the equation has the form

$$wb1 = wb \times s1$$

where $wb1$ denotes a budding rate of vesicles that transfer from the Golgi apparatus to the tube tip initiated by GTPase B, wb denotes a constant unique to GTPase B, and $s1$ denotes the area of the Golgi apparatus. Let wa be a constant unique to GTPase A that initiates vesicle budding from the tube tip and directs the vesicles to the Golgi apparatus. Then, $wb = 1$ and $wa = 0.01$.

(6) When SNAREs are recruited from a compartment to vesicles, SNAREs that are not native to the compartment are recruited more than those native to the compartment (i.e. when vesicles bud from the Golgi apparatus, SNARE Y, V, Z, and W are recruited to a vesicle at a 100-fold higher frequency than SNARE X and U. This difference was mathematically identified by Heinrich and Rapoport (2005), which allows the system to reach equilibrium. Consequently, the equation has the form

$$sxb = \frac{\frac{x1}{kxb}}{\left(1 + \frac{x1}{kxb} + \frac{u1}{kub} + \frac{y1}{kyb} + \frac{v1}{kvb} + \frac{z1}{kzb} + \frac{w1}{kwb}\right)}$$

where sxb denotes a saturation function for carrying SNARE X to vesicles that are initiated by GTPase B; $x1$, $u1$, $y1$, $v1$, $z1$, and $w1$ denote concentrations of SNARE X, U, Y, V, Z, and W at the Golgi apparatus, respectively; and kxb , kub , kyb , kvb , kzb , and kwb denote relative dissociation constants (reverse numbers of recruitment rates) of SNARE X, U, Y, V, Z, and W for GTPase B, respectively. $kxb = kub = 100$ and $kyb = kvb = kzb = kwb = 1$.

(7) The rate of vesicle fusion depends on the concentration of interaction pairs of v-SNAREs and t-SNAREs in vesicles and a compartment. Therefore, the equation takes the form

$$fb2 = K(xb1 \times u2 + ub1 \times x2 + yb1 \times v2 + vb1 \times y2 + zb1 \times w2 + wb1 \times z2)$$

where $fb2$ denotes a fusion frequency of vesicles from the Golgi apparatus to the tube tip; K denotes a constant; $xb1$, $ub1$, $yb1$, $vb1$, $zb1$, and $wb1$ denote concentrations of SNARE X, U, Y, V, Z, and W in vesicles budded from the Golgi apparatus by GTPase B, respectively; and $u2$, $x2$, $v2$, $y2$, $w2$, and $z2$ denote concentrations of SNARE U, X, V, Y, W, and Z in the tube tip, respectively. $K = 40$.

(8) The vast majority of membranes and SNAREs that are required for the vesicle trafficking are accumulated in the Golgi apparatus at the initiation of a pollen tube ($t = t_0$; Fig. 2B). At a certain point in time ($t = t_s$), vesicle trafficking among the Golgi apparatus, tube tip, and recycling endosome reaches equilibrium. Consequently, initial conditions include

$$s1(0) = 0.96, \quad s2(0) = s3(0) = nb1(0) = ne1(0) = na2(0) = nd2(0) = nc3(0) = nf3(0) = 0.005$$

where $s1(0)$, $s2(0)$, and $s3(0)$ are relative compartment areas of the Golgi apparatus, tube tip, and recycling endosome at a pollen tube initiation ($t = t_0$), respectively. $nb1(0)$, $ne1(0)$, $na2(0)$, $nd2(0)$, $nc3(0)$, and $nf3(0)$ are total vesicle areas budded from the Golgi apparatus, tube tip, and recycling

endosome by GTPases B, E, A, D, C, and F, respectively, at the initiation of a pollen tube ($t = t_0$), respectively. The total relative area of compartments and vesicles is 1.

(9) All pectin and cargo phospholipids that are required for pollen tube elongation are already synthesized in the Golgi apparatus at time 0 and delivered to the tube tip through vesicle trafficking as a function of time (Fig. 2B).

(10) The amount of pectin that vesicles can carry depends on a concentration of pectin in a compartment and a recruitment rate defined by a specific GTPase. Vesicles initiated by small GTPases at the tube tip do not carry pectin. Hence, the equation has the form

$$spb1 = \frac{p1}{1 + \frac{p1}{kpb}}$$

where $spb1$ denotes the saturation function for carrying pectin in vesicles initiated by GTPase B, $p1$ denotes the concentration of pectin in the Golgi apparatus, and kpb denotes the relative dissociation constant (the reverse number of the pectin recruitment rate) for GTPase B. Let $1/kpd$ be a pectin recruitment rate of GTPase D. Then, $1/kpb = 0.01$ and $1/kpd = 0$. The total amount of pectin in the cell is always 1.

(11) Phospholipids in the vesicle trafficking system and those to expand the plasma membrane are distinguished. Phospholipids to expand the plasma membrane are considered as cargos (designated cargo phospholipids; Supplemental Figs. S1 and S2). The amount of the cargo phospholipids that vesicles can carry depends on only the concentration in the compartment. Vesicles initiated at the tube tip do not carry the cargo phospholipids. Hence, the equation has the form

$$shb1 = \text{buffer} \times \frac{h1}{1 + h1}$$

where $shb1$ denotes a saturation function for carrying cargo phospholipids in vesicles initiated by GTPase B, buffer denotes a constant (0.03), and $h1$ denotes the concentration of cargo phospholipids in the Golgi apparatus. Let $shd2$ be a saturation function for carrying cargo phospholipids in vesicles initiated by GTPase D. Then, $shd2 = 0$. The total amount of cargo phospholipids in the cell is always 1.

(12) The tube length is defined by the amount of pectin and cargo phospholipids transported to the tube tip. Hence, the differential equation has the form

$$\frac{dl}{dt} = \sqrt{(mpb1 + mpc3)(mhb1 + mhc3)}$$

where dl/dt denotes the rate of tube growth and $mpb1$, $mpc3$, $mhb1$, and $mhc3$ denote pectin and cargo phospholipids delivered to the tube tip from the Golgi apparatus and recycling endosome, respectively. The maximum length is 1.

Differential equations that describe our assumption were established and proved that the vesicle trafficking reaches equilibrium with the variables and constants we used (Supplemental Proof S1).

Computation

Codes in the ODE file made by Heinrich and Rapoport (2005) were modified based on our assumptions (Supplemental Program S1). The XPPAUT 5.98 program (<http://www.math.pitt.edu/~bard/xpp/xpp.html/>) was used to compute the differential equations. The results were exported to Microsoft Excel files, and the graphs were generated in the files.

Supplemental Data

The following materials are available in the online version of this article.

Supplemental Figure S1. Vesicle composition in the mathematical model.

Supplemental Figure S2. Exocytosis and endocytosis in the mathematical model.

Supplemental Figure S3. Predicted changes of the concentrations of pectin and cargo phospholipids in vesicles.

Supplemental Figure S4. Predicted changes of SYP125 and pectin amounts at the tube tip.

Supplemental Table S1. List of the vesicle trafficking genes.

Supplemental Proof S1. Mathematical proof of vesicle trafficking equilibrium.

Supplemental Program S1. Differential equations of vesicle trafficking.

ACKNOWLEDGMENT

We thank Dr. Bret Elderd for critical reading of the manuscript.

Received October 2, 2009; accepted November 16, 2009; published November 20, 2009.

LITERATURE CITED

- Achard P, Herr A, Baulcombe DC, Harberd NP (2004) Modulation of floral development by a gibberellin-regulated microRNA. *Development* **131**: 3357–3365
- Allen RS, Li J, Stahle MI, Dubroue A, Gubler F, Millar AA (2007) Genetic analysis reveals functional redundancy and the major target genes of the Arabidopsis miR159 family. *Proc Natl Acad Sci USA* **104**: 16371–16376
- Anders N, Jurgens G (2008) Large ARF guanine nucleotide exchange factors in membrane trafficking. *Cell Mol Life Sci* **65**: 3433–3445
- Behnia R, Munro S (2005) Organelle identity and the signposts for membrane traffic. *Nature* **438**: 597–604
- Benli M, Doring F, Robinson DG, Yang X, Gallwitz D (1996) Two GTPase isoforms, Ypt31p and Ypt32p, are essential for Golgi function in yeast. *EMBO J* **15**: 6460–6475
- Boavida LC, McCormick S (2007) Temperature as a determinant factor for increased and reproducible in vitro pollen germination in Arabidopsis thaliana. *Plant J* **52**: 570–582
- Boavida LC, Shuai B, Yu HJ, Pagnussat GC, Sundaresan V, McCormick S (2009) A collection of Ds insertional mutants associated with defects in male gametophyte development and function in Arabidopsis thaliana. *Genetics* **181**: 1369–1385
- Boehm M, Bonifacino JS (2001) Adaptins: the final recount. *Mol Biol Cell* **12**: 2907–2920
- Borges F, Gomes G, Gardner R, Moreno N, McCormick S, Feijo JA, Becker JD (2008) Comparative transcriptomics of Arabidopsis sperm cells. *Plant Physiol* **148**: 1168–1181
- Bove J, Vaillancourt B, Kroeger J, Hepler PK, Wiseman PW, Geitmann A (2008) Magnitude and direction of vesicle dynamics in growing pollen tubes using spatiotemporal image correlation spectroscopy and fluorescence recovery after photobleaching. *Plant Physiol* **147**: 1646–1658
- Cai G, Cresti M (2009) Organelle motility in the pollen tube: a tale of 20 years. *J Exp Bot* **60**: 495–508
- Cai H, Reinisch K, Ferro-Novick S (2007) Coats, tethers, Rabs, and SNAREs work together to mediate the intracellular destination of a transport vesicle. *Dev Cell* **12**: 671–682
- Cao D, Cheng H, Wu W, Soo HM, Peng J (2006) Gibberellin mobilizes distinct DELLA-dependent transcriptomes to regulate seed germination and floral development in Arabidopsis. *Plant Physiol* **142**: 509–525
- Carr CM, Novick PJ (2000) Membrane fusion: changing partners. *Nature* **404**: 347–349
- Chen CY, Balch WE (2006) The Hsp90 chaperone complex regulates GDI-dependent Rab recycling. *Mol Biol Cell* **17**: 3494–3507
- Cheng H, Qin L, Lee S, Fu X, Richards DE, Cao D, Luo D, Harberd NP, Peng J (2004) Gibberellin regulates Arabidopsis floral development via suppression of DELLA protein function. *Development* **131**: 1055–1064
- Chhun T, Aya K, Asano K, Yamamoto E, Morinaka Y, Watanabe M, Kitano H, Ashikari M, Matsuoka M, Ueguchi-Tanaka M (2007) Gibberellin regulates pollen viability and pollen tube growth in rice. *Plant Cell* **19**: 3876–3888
- Cole RA, Synek L, Zarsky V, Fowler JE (2005) SEC8, a subunit of the putative Arabidopsis exocyst complex, facilitates pollen germination and competitive pollen tube growth. *Plant Physiol* **138**: 2005–2018
- Derksen J, Knuiman B, Hoedemaekers K, Guyon A, Bonhomme S, Pierson ES (2002) Growth and cellular organization of Arabidopsis pollen tubes in vitro. *Sex Plant Reprod* **15**: 133–139

- Derksen J, Rutten T, Lichtscheidl IK, de Win AHN, Pierson ES, Rongen G (1995) Quantitative analysis of the distribution of organelles in tobacco pollen tubes: implications for exocytosis and endocytosis. *Protoplasma* **188**: 267–276
- Elias M, Drdova E, Ziak D, Bavlanka B, Hala M, Cvrckova F, Soukupova H, Zarsky V (2003) The exocyst complex in plants. *Cell Biol Int* **27**: 199–201
- Enami K, Ichikawa M, Uemura T, Kutsuna N, Hasezawa S, Nakagawa T, Nakano A, Sato MH (2009) Differential expression control and polarized distribution of plasma membrane-resident SYP1 SNAREs in *Arabidopsis thaliana*. *Plant Cell Physiol* **50**: 280–289
- Fujiki Y, Yoshimoto K, Ohsumi Y (2007) An *Arabidopsis* homolog of yeast ATG6/VPS30 is essential for pollen germination. *Plant Physiol* **143**: 1132–1139
- Grosshans BL, Ortiz D, Novick P (2006) Rabs and their effectors: achieving specificity in membrane traffic. *Proc Natl Acad Sci USA* **103**: 11821–11827
- Hala M, Cole R, Synek L, Drdova E, Pecenkova T, Nordheim A, Lamkemeyer T, Madlung J, Hochholdinger F, Fowler JE, et al (2008) An exocyst complex functions in plant cell growth in *Arabidopsis* and tobacco. *Plant Cell* **20**: 1330–1345
- He B, Guo W (2009) The exocyst complex in polarized exocytosis. *Curr Opin Cell Biol* **21**: 537–542
- Heinrich R, Rapoport TA (2005) Generation of nonidentical compartments in vesicular transport systems. *J Cell Biol* **168**: 271–280
- Hofmann KP, Spahn CM, Heinrich R, Heinemann U (2006) Building functional modules from molecular interactions. *Trends Biochem Sci* **31**: 497–508
- Honys D, Twell D (2004) Transcriptome analysis of haploid male gametophyte development in *Arabidopsis*. *Genome Biol* **5**: R85
- Hruz T, Laule O, Szabo G, Wessendorp F, Bleuler S, Oertle L, Widmayer P, Gruissem W, Zimmermann P (2008) Genevestigator V3: a reference expression database for the meta-analysis of transcriptomes. *Adv Bioinformatics* **2008**: 420747
- Ischebeck T, Stenzel I, Heilmann I (2008) Type B phosphatidylinositol-4-phosphate 5-kinases mediate *Arabidopsis* and *Nicotiana tabacum* pollen tube growth by regulating apical pectin secretion. *Plant Cell* **20**: 3312–3330
- Jakobsen MK, Poulsen LR, Schulz A, Fleurat-Lessard P, Moller A, Husted S, Schiott M, Amtmann A, Palmgren MG (2005) Pollen development and fertilization in *Arabidopsis* is dependent on the MALE GAMETOGENESIS IMPAIRED ANthers gene encoding a type V P-type ATPase. *Genes Dev* **19**: 2757–2769
- Jedd G, Mulholland J, Segev N (1997) Two new Ypt GTPases are required for exit from the yeast trans-Golgi compartment. *J Cell Biol* **137**: 563–580
- Kaneko M, Inukai Y, Ueguchi-Tanaka M, Itoh H, Izawa T, Kobayashi Y, Hattori T, Miyao A, Hirochika H, Ashikari M, et al (2004) Loss-of-function mutations of the rice GAMYB gene impair α -amylase expression in aleurone and flower development. *Plant Cell* **16**: 33–44
- Ketelaar T, Galway ME, Mulder BM, Emons AM (2008) Rates of exocytosis and endocytosis in *Arabidopsis* root hairs and pollen tubes. *J Microsc* **231**: 265–273
- Kitano H (2002) Systems biology: a brief overview. *Science* **295**: 1662–1664
- Kroeger JH, Geitmann A, Grant M (2008) Model for calcium dependent oscillatory growth in pollen tubes. *J Theor Biol* **253**: 363–374
- Lam SK, Tse YC, Robinson DG, Jiang L (2007) Tracking down the elusive early endosome. *Trends Plant Sci* **12**: 497–505
- Lee Y, Kim ES, Choi Y, Hwang I, Staiger CJ, Chung YY (2008) The *Arabidopsis* phosphatidylinositol 3-kinase is important for pollen development. *Plant Physiol* **147**: 1886–1897
- Lee YJ, Yang Z (2008) Tip growth: signaling in the apical dome. *Curr Opin Plant Biol* **11**: 662–671
- Lin WH, Ye R, Ma H, Xu ZH, Xue HW (2004) DNA chip-based expression profile analysis indicates involvement of the phosphatidylinositol signaling pathway in multiple plant responses to hormone and abiotic treatments. *Cell Res* **14**: 34–45
- Markgraf DF, Peplowska K, Ungermann C (2007) Rab cascades and tethering factors in the endomembrane system. *FEBS Lett* **581**: 2125–2130
- Moscatelli A, Ciampolini F, Rodighiero S, Onelli E, Cresti M, Santo N, Idilli A (2007) Distinct endocytic pathways identified in tobacco pollen tubes using charged nanogold. *J Cell Sci* **120**: 3804–3819
- Otegui MS, Spitzer C (2008) Endosomal functions in plants. *Traffic* **9**: 1589–1598
- Paul MJ, Frigerio L (2007) Coated vesicles in plant cells. *Semin Cell Dev Biol* **18**: 471–478
- Pina C, Pinto F, Feijo JA, Becker JD (2005) Gene family analysis of the *Arabidopsis* pollen transcriptome reveals biological implications for cell growth, division control, and gene expression regulation. *Plant Physiol* **138**: 744–756
- Ridley AJ (2006) Rho GTPases and actin dynamics in membrane protrusions and vesicle trafficking. *Trends Cell Biol* **16**: 522–529
- Robinson DG, Jiang L, Schumacher K (2008) The endosomal system of plants: charting new and familiar territories. *Plant Physiol* **147**: 1482–1492
- Rojo E, Denecke J (2008) What is moving in the secretory pathway of plants? *Plant Physiol* **147**: 1493–1503
- Samaj J, Muller J, Beck M, Bohm N, Menzel D (2006) Vesicular trafficking, cytoskeleton and signalling in root hairs and pollen tubes. *Trends Plant Sci* **11**: 594–600
- Samaj J, Read ND, Volkmann D, Menzel D, Baluska F (2005) The endocytic network in plants. *Trends Cell Biol* **15**: 425–433
- Sanderfoot A, Raikhel N (2003) The secretory system of *Arabidopsis*. In *The Arabidopsis Book*. American Society of Plant Biologists, Rockville, MD, doi/, <http://www.aspb.org/publications/arabidopsis/>
- Sangster TA, Bahrami A, Wilczek A, Watanabe E, Schellenberg K, McLellan C, Kelley A, Kong SW, Queitsch C, Lindquist S (2007) Phenotypic diversity and altered environmental plasticity in *Arabidopsis thaliana* with reduced Hsp90 levels. *PLoS One* **2**: e648
- Schmid EM, McMahon HT (2007) Integrating molecular and network biology to decode endocytosis. *Nature* **448**: 883–888
- Schwab R, Palatnik JF, Riester M, Schommer C, Schmid M, Weigel D (2005) Specific effects of microRNAs on the plant transcriptome. *Dev Cell* **8**: 517–527
- Seabra MC, Wasmeier C (2004) Controlling the location and activation of Rab GTPases. *Curr Opin Cell Biol* **16**: 451–457
- Silverstone AL, Mak PY, Martinez EC, Sun TP (1997) The new RGA locus encodes a negative regulator of gibberellin response in *Arabidopsis thaliana*. *Genetics* **146**: 1087–1099
- Sorensen JB, Wiederhold K, Muller EM, Milosevic I, Nagy G, de Groot BL, Grubmuller H, Fasshauer D (2006) Sequential N- to C-terminal SNARE complex assembly drives priming and fusion of secretory vesicles. *EMBO J* **25**: 955–966
- Sousa E, Kost B, Malho R (2008) *Arabidopsis* phosphatidylinositol-4-monophosphate 5-kinase 4 regulates pollen tube growth and polarity by modulating membrane recycling. *Plant Cell* **20**: 3050–3064
- Stein A, Weber G, Wahl MC, Jahn R (2009) Helical extension of the neuronal SNARE complex into the membrane. *Nature* **460**: 525–528
- Synek L, Schlager N, Elias M, Quentin M, Hauser MT, Zarsky V (2006) ATEXO70A1, a member of a family of putative exocyst subunits specifically expanded in land plants, is important for polar growth and plant development. *Plant J* **48**: 54–72
- Szumlanski AL, Nielsen E (2009) The Rab GTPase RabA4d regulates pollen tube tip growth in *Arabidopsis thaliana*. *Plant Cell* **21**: 526–544
- Tsuji H, Aya K, Ueguchi-Tanaka M, Shimada Y, Nakazono M, Watanabe R, Nishizawa NK, Gomi K, Shimada A, Kitano H, et al (2006) GAMYB controls different sets of genes and is differentially regulated by microRNA in aleurone cells and anthers. *Plant J* **47**: 427–444
- Van Damme D, Coutuer S, De Rycke R, Bouget FY, Inze D, Geelen D (2006) Somatic cytokinesis and pollen maturation in *Arabidopsis* depend on TPLATE, which has domains similar to coat proteins. *Plant Cell* **18**: 3502–3518
- Vernoud V, Horton AC, Yang Z, Nielsen E (2003) Analysis of the small GTPase gene superfamily of *Arabidopsis*. *Plant Physiol* **131**: 1191–1208
- Wang Y, Zhang WZ, Song LF, Zou JJ, Su Z, Wu WH (2008) Transcriptome analyses show changes in gene expression to accompany pollen germination and tube growth in *Arabidopsis*. *Plant Physiol* **148**: 1201–1211
- Yoshizawa AC, Kawashima S, Okuda S, Fujita M, Itoh M, Moriya Y, Hattori M, Kanehisa M (2006) Extracting sequence motifs and the phylogenetic features of SNARE-dependent membrane traffic. *Traffic* **7**: 1104–1118
- Zonia L, Munnik T (2008) Vesicle trafficking dynamics and visualization of zones of exocytosis and endocytosis in tobacco pollen tubes. *J Exp Bot* **59**: 861–873